Micro-Patterning onto DLC coating by Plasma Oxygen Etching

ICOMM 2012 No. 1

Tatsuhiko Aizawa[1], E. E. Yunata[2], N. T. Redationo[3] and Tatsuya Fukuda[4]
[1]Dept. Design and Engr., Shibaura Institute of Technology, Japan; e-mail: taizawa@sic.shibaura-it.ac.jp
[2]Graduate School, Department of Physics, Brawijaya University, Indonesia; e-mail: erzyy@yahoo.co.id
[3]Graduate School, Department of Mechanical Engineering, Brawijaya University, Indonesia; e-mail: veneture2@yahoo.com
[4]R & D Center, Mitsue Mold Engineering, Co., Ltd., Japan; e-mail: fukuda@mitue.co.jp

ABSTRACT

Micro- and nano-patterning to coated substrates becomes popular for fabricating the tools and dies to imprint the designed patterns onto optical polymers and oxide glasses and for fabricating the micro-devices. In particular, DLC-coated tools and dies have sufficient strength and wear-toughness enough to be working as a mold-die for imprinting these patterns onto any optical materials even at the elevated temperature. In the present paper, high density oxygen plasma etching system is developed to make high-speed etching onto DLC coated mold materials. With aid of in-situ plasma diagnosis, the whole etching process from initial state to termination is on-line monitored to describe the etching behavior. Owing to the activated oxygen atom flux, high etching rate is attained in the present system; e.g., about 13.7 μm/H only for DLC coating without any interlayers or top/under coatings, and, around 5.0 μm/H at the presence of thin metallic interlayers. Micro-grooving patterns are utilized to investigate the effect of micro-geometry on the accuracy of etching.

INTRODUCTION

Diamond-like-carbon coating (DLC coating) has been widely used as a protective coating for tools and dies. In particular, this kind of protection is indispensable for die-materials to be used in mold-stamping of oxide glasses into optical elements even at the elevated temperature [1]. Owing to improvement of thermal stability, tooling life in mold-dies is significantly extended with success by using the metal-doped DLC coating [2-3]. Furthermore, DOE (Diffractive Optical Element) or MAL (Multi-Arrayed Lens) requires for fine patterning onto the mold-die; e.g. Fresnel patterning for DOE [4]. Hence, micro-pattering onto DLC coating provides us a solution of new mold-dies for mold-stamping of DOE and MAL. As had been discussed in [5-6], there are three methods to make micro-patterning onto DLC coated tools and dies. In the conventional mechanical machining, micro-patterns must be first fine-machined onto the substrate materials before DLC coating; resolution in patterning is strictly limited by 50 to 100 μm. Short-time pulse laser machining is also useful to make patterning directly on the DLC coating [7-9]. Plasma oxygen etching method is favored by precise, fine micro-patterning also directly onto the DLC coating [10-13].

In the present paper, our developing high density RF-DC plasma oxygen etching system is introduced to make fine etching without use of hazardous chemical etchants. Plasma diagnosis with aid of spectroscopic measurement helps us, not only to understand the oxygen plasma state in etching process but also to describe the plasma etching behavior via in-situ spectroscopic measurement. Chromium-masked DLC-coated SKD11 specimens are prepared to investigate the oxygen-plasma etching process for various micro-grooving patterns with different line widths and pitches.

Owing to the activated oxygen atom flux, high etching rate is attained in the present system; e.g., it is about 13.7 μm/H only for DLC coating without any interlayers or top/under coatings, and, around 5.0 μm/H, at the presence of thin chromium and amorphous silicon carbide (SiC) interlayers. Micro-grooving patterns with the line width from 3 μm to 100 μm are utilized to investigate the effect of micro-geometry on the accuracy of etching. Precise measurement of surface profiles proves sufficient accuracy in the present micro-patterning.

EXPERIMENTAL PROCEDURE

Our developing plasma etching system equipped with spectroscopic measurement is introduced to understand the difference from the conventional plasma etching approaches. The specimens for micro-patterning are also prepared not only to measure the etching rate of DLC coating but also to investigate the effect of micro-geometry on the accuracy in micro-patterning.

A. PLASMA ETCHING SYSTEM

RF-DC plasma etching system was developed to investigate the optimum condition for etching of carbon-based materials including DLC coatings, as shown in Figure 1. Different from the conventional DC- or RF-plasma generators, there is no mechanical matching box; input and out powers are automatically matched by frequency adjustment around 2 MHz. This difference reflects on the response against temporally varying plasma states. The conventional mechanical matching requires for the duration time in the order of 1s to 10 s to adjust the RF-power. While, in the present system, it is shortened down to 1 ms; i.e. there is no time delay for power control to drive the etching process in the present system.

In In addition, the chamber is electrically neutral so that RF and DC are controlled independently from each other.

RF-voltage is controlled up to 250 V, while DC bias, down to - 600 V. A dipole electrode is utilized to generate RF-plasma; DC bias is directly applied to the specimens. Heating unit is also located under this DC-biased plate.

The normal operation in experiments is stated as follows. After evacuation down to the base pressure of 0.1 Pa, a carrier gas was introduced into the chamber to attain the specified pressure. Both oxygen and argon gases are available in this system besides the nitrogen gas for bent. With use of magnetic lens, the ignited RF-DC oxygen plasmas were focused onto the surface of specimens during etching. After preliminary experiments, RF-voltage, DC bias and pressure was selected to be 250 V, -450 V and 25 to 40 Pa, respectively in the following experiments. The effect of RF- and DC-voltages on the etching behavior is discussed through the spectroscopic measurement. Carrier gas pressure has direct influence on the etching rate to be discussed later.

Fig.1: High density plasma etching system. 1: Chamber, 2: RF-plasma generator, 3: Control-panel, 4: Electric sources, 5: Evacuation system, 6: Gas supply.

B. PLASMA ETCHING EXPERIMENTA SET-UP

Different from the conventional plasma system, spatial geometric configuration of plasmas is also controlled by set-up of dipole electrode, cathode plate and magnetic lens, as depicted in Fig. 2. Optimum experimental set-up was determined by using the plasma diagnosis.

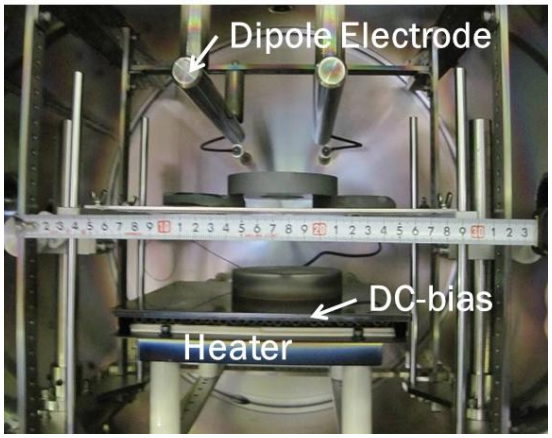

Fig. 2: Experimental set-up in this plasma etching system.

C. PLSAMA DISGNOSIS

Activated state of oxygen plasmas was described by using the spectroscopic measurement. As depicted in Fig. 3, light emission from plasmas was introduced through the fiber-scope with narrowed aperture and analyzed by spectroscopy (Hamamatsu Photonics, Co. Ltd.). Emissive light was detected via the silica window; there is no external disturbance in the measured spectrum from the experimental set-up in Fig. 3.

To be discussed in later, the activated species have all their characteristic peak profile at the specified wave length. Each peak is identified as the corresponding to species by citing the database [14]. In the case of oxygen plasma state, activated oxygen molecules (O_2*) and atoms (O*) coexist with ionized oxygen molecules and atoms.

In addition, chemical reaction during plasma etching was also in-situ monitored by this system. New peaks corresponding to the reactants often overlap with the above peaks of activated species in the measured spectra. In the following measurement, rational decomposition algorithm was utilized to separate each characteristics peak from spectra and to identify each decomposed peak by citing [14] and references [15-16].

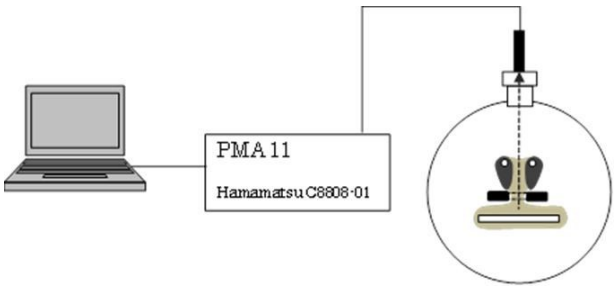

Fig. 3: Illustration of plasma diagnosis instrumentation attached to the present plasma etching system.

D. SPECIMENS

Two types of specimens were employed in this experiment. DLC-coated WC (Co) specimen without any interlayers, was used for measurement of etching rate. The chromium-masked SKD-11 specimen was also used to investigate the effect of micro-groove pattern on the etching behavior. Figure 4 illustrates the chromium masking method; the specimen has sandwich-structure of three layers: 1) undercoat of amorphous silicon carbide with the thickness of 10 nm (a-SiC) and chromium layer with the thickness of 100 nm, 2) main-DLC coating with the thickness around 5 μm, and, 3) top-coat of a-SiC and chromium mask with the thickness of 100 nm.

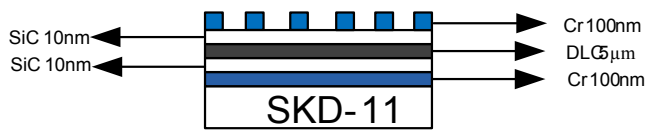

Fig. 4: Sandwich structure of coating in the Cr-masked specimen.

Fig. 5 Chromium masked SKD-11 specimen with variety of micro-groove pattern in the masking.

As shown in Fig. 5, many standard micro-patterns were printed onto the a-SiC capped DLC coating; e.g. the micro-groove width was varied from 3 μm to 100 μm. Since the film thickness of DLC coating is 5 μm, this variation is equivalent to the change of aspect ratio in micro-grooving from 1.67 to 0.05. When using the Cr-interlayered DLC coating, the etching rate might be retarded by relatively thick chromium interlayer. In the latter specimen, the measured etching rate might be affected by the a-SiC top coat.

EXPERIMENTAL RESULTS

A. PLASMA DISGNOSIS OF OXYGEN PLASMA

Various kinds of species are always activated in the plasma state, where each species has some amount of peak intensity at the characteristic wave length in the emission spectrum. Hence, each plasma state, which is controlled by various processing parameters, has characteristic spectrum of activated species in the function of wave-length.

In case of oxygen plasmas generated under the present RF-DC control, they are classified by two typical states; i.e. molecular species governing state, and, atomic or ionic species governing state. In the former, the activated oxygen molecules (O_2*) is a main component in the emission spectrum as shown in Fig. 6. Most of species are present in the relatively lower wave length and little peaks are seen in the longer wave length. Activated oxygen atoms (O*) are certainly present together with O_2*; however their intensities are smaller than those of O_2*. This coexistence of OII, OIII and OIV activated oxygen atoms with O_2* is characteristic to this molecule governing plasma state in Fig. 6.

This molecule governing state of plasmas changes itself to oxygen atom governing state. As shown in Fig. 7, strong peaks are seen in the relatively long wave length range; those are O* (OIV) at 866 nm and O_2^+ at 774 nm, respectively. In addition, there are two differences between these oxygen molecule and atom governing states. First, the peak intensity of OIV is enhanced together with OIII and OII in the oxygen atomic species. O_2^+ has the strongest peak among the activated species. This implies that most of molecular oxygen is once activated to O_2^+ and then decomposed to various oxygen atoms with different covalent numbers.

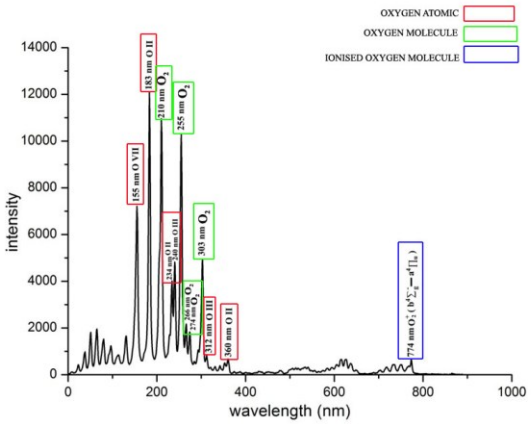

Fig. 6: Oxygen molecule governing state of plasmas.

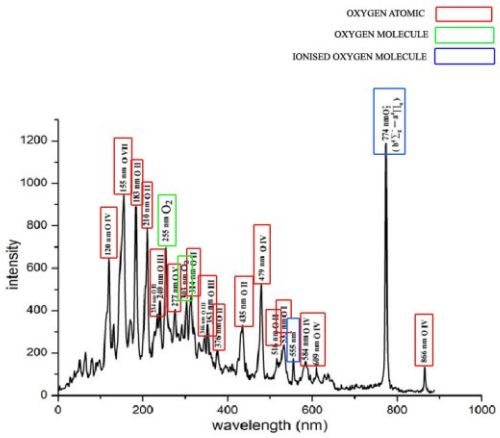

Fig. 7: Oxygen atom governing state of plasmas.

Hence, this change of plasma state is driven by increase of the electron density in the plasmas by intense ionization of oxygen atoms and molecules. In practice, the above oxygen atom governing plasma state is preferable to make oxygen plasma etching of DLC coating, to be discussed later.

B. IN-SITUE DIAGNOSIS DURING PLASMA ETCHING

The measured plasma state in Figs. 6 and 7 might change itself during the plasma etching of DLC coating, because of direct chemical reaction between activated oxygen atoms in the plasmas and carbon atoms in DLC coating. Then, in-situ detection of reactants in this direct reaction must be the first step to describe this oxygen plasma etching behavior. There are several reaction routes to remove the carbon in DLC coating during etching; e.g. $C + O_2^* \rightarrow CO_2$, $C + O_2^+ + e \rightarrow CO_2$, or, $C + O^* \rightarrow CO$.

Figure 8 shows the in-situ measured spectrum in the shorter wave length range during plasma etching. Besides activated oxygen atoms, several peaks corresponding to carbon mono-oxide (or CO) were detected.

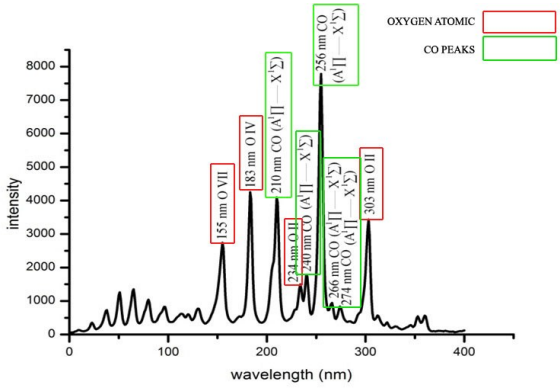

Fig. 8: Typical spectrum in-situ measured during plasma etching process.

This in-situ detection of CO-peaks proves that direction reaction of carbon atoms in the DLC film with oxygen atoms from plasmas should drive the etching process to remove carbon atoms from DLC films. This implies that the similar reaction might take place to remove the metallic or ceramic layers via generation of metallic mono-oxides.

C. ETCHING RATE MEASUREMENT

DLC-coated SKD-11 specimen with thick chromium interlayer was first used to make the total etching rate. Figure 9 depicts the specimen surface after plasma etching for 290 s. The left half of specimens was masked by polyimide tape; the right half was only subjected to this plasma etching. The right half of DLC coating with the thickness of 1.1 μm was completely removed during this duration; i.e. the etching rate of DLC coating is estimated to be 3.8 nm/s, or, 13.7 μm/H.

Fig. 9: DLC-coated SKD-11 samples without any interlayers.

When using the chromium masked DLC coating, this etching rate might be retarded by the presence of top coat of a-SiC or chromium residuals; etching process of DLC coating is expected to be terminated by the presence of under-coat. DLC coating with the thickness of 5 μm was etched into micro-grooving patterns within 3520 s; the average etching rate is 5 μm/H. In fact, this retardation of etching process is mainly attributed to a-SiC top coat.

D. MICRO-PATTERNING

The chromium masking pattern on the surface of specimen in Fig. 5, was first compared before and after plasma etching. In general, the metallic masks are easy to be timbered with increasing the aspect ratio of pattern depth to pattern width in the etching process. As shown in Fig. 10, no change of patterns during plasma etching was seen in optical microscopic observation. This proves that no damage should occur by this oxygen plasma etching; the geometric accuracy of micro-grooves might be preserved on the surface. Figure 11 shows a typical SEM image of micro-patterned DLC coating.

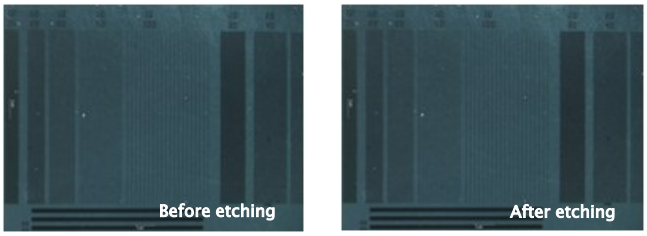

Fig. 10: Comparison of chromium-etched pattern on the surface of specimens before and after plasma etching.

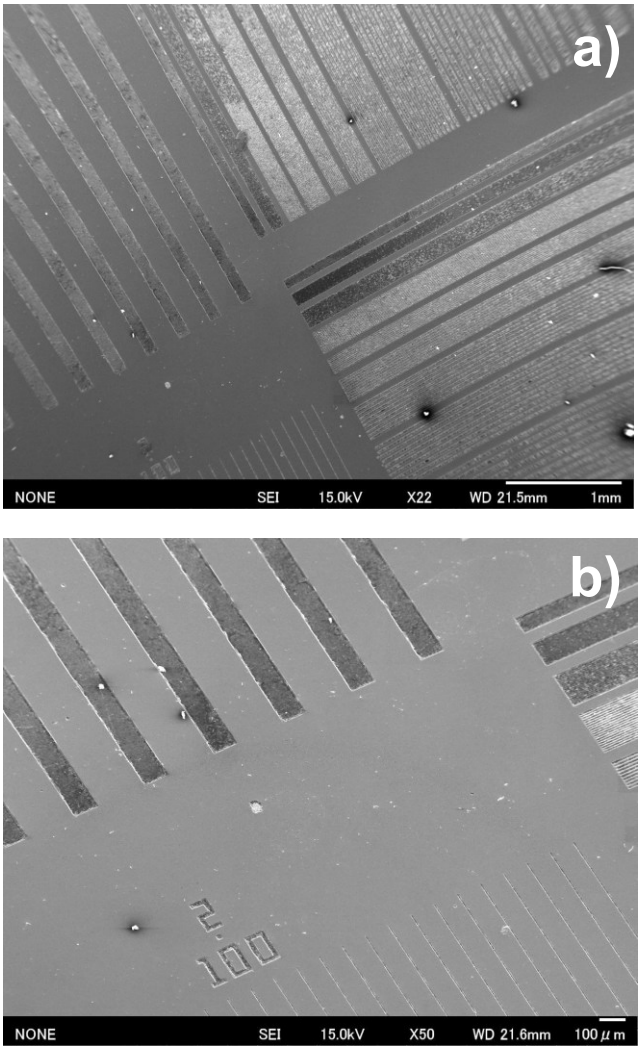

Fig. 11: SEM image of micro-patterns onto the DLC coatings by the oxygen plasma etching.

Various micro-grooving patterns were simultaneously etched onto DLC coating as shown in Fig. 11 a). Homogeneous etching took place irrespective of the groove widths and pitches. With degreasing the grooving width down to 3 μm, the aspect-ratio becomes more than 1.0, so that DLC-wall of pattern between adjacent grooves becomes so thin to be timbered down during etching. In fact, these thin DLC-walls were timbered and etched all together when the micro-grooving pitch becomes less than 5 μm in Fig. 11 b). Hence, DC bias must be controlled to be lower enough to be free from over-etching. Owing to a series of experiments, DC bias might well be controlled to be less than – 250 V.

The depth profiles of micro grooves in details were measured by using the laser profilometer (NH-3SP; Mitaka-Kouki, Co. Ltd.). Figure 12 shows a typical micro-grooving pattern when using the micro-groove mask with the width (W_G) of 100 μm and the pitch (P_G) of 200 μm. The absolute value of measured depth is correct by laser reflection; some noises are inevitably included in measurement. Since the etching process is terminated by under-coat of chromium and amorphous SiC layers, the whole of un-masked DLC coating was completely removed to make micro-grooves as designed. Their average groove width at the bottom was measured to become around 98 μm, and, their average pitch, around 200 μm. This agreement between designed and measured W_G and P_G proves that micro-patterning should take place with sufficient accuracy by the present oxygen plasma etching. The side surfaces of etched micro-grooves become smooth and stand steep against the bottom surface; this geometry is preferable to mold-die technology.

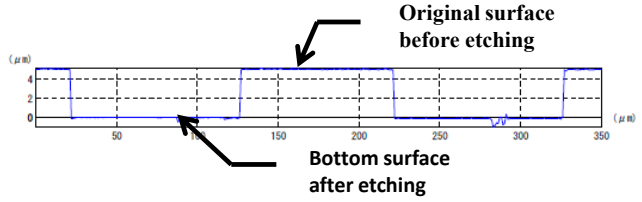

Fig. 12: Depth profile of micro-grooving pattern, plasma-etched onto the DLC coating when using the Cr-grooving pattern with W_G = 100 μm and P_G = 200 μm.

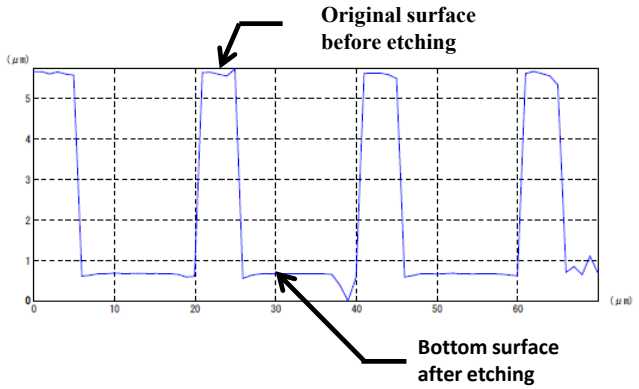

Fig. 13: Depth profile of micro-grooving pattern, etched onto the DLC coating by W_G = 5 μm and P_G = 20 μm.

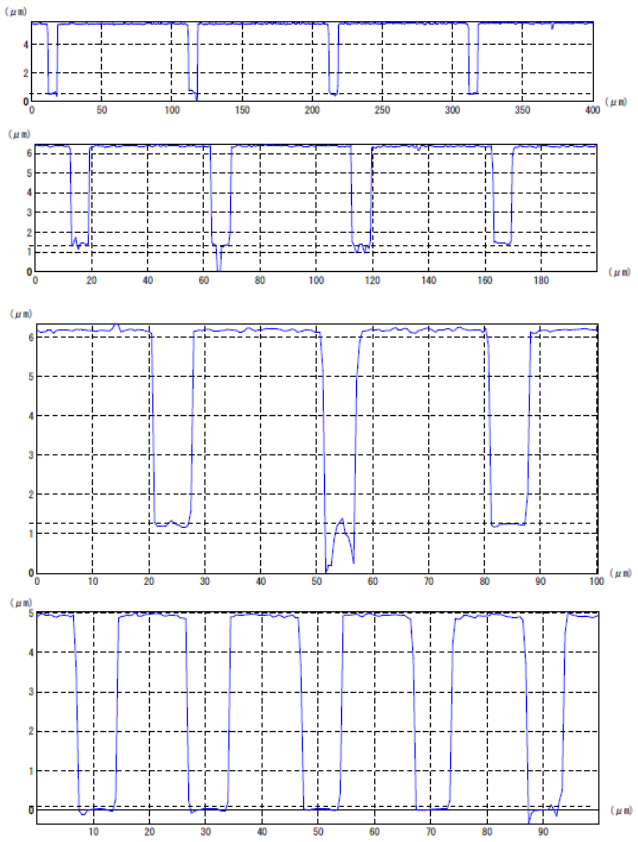

Fig. 14: Depth profile of micro-grooves for various pitches with their width kept constant by 6 μm in the initial chromium masking.

Next, let us investigate the effect of groove width in the Cr-grooving pattern on the etching behavior. Figure 13 depicts the depth profile in micro-grooving when W_G = 5 μm and P_G = 20 μm. Although a part of chromium top-coat in the masking pattern was etched and curved, both the edges and bottom in the micro-groove were formed with sufficient sharpness and straightforwardness. In the case of Fig. 13, the averages of W_G and P_G were 4.5 μm and 20 μm; this shortness of W_G is attributed to over-etching on the top-coat.

Effect of pitch (P_G) in micro-pattern on the etching behavior was investigated with the width of groove kept constant by 6 μm in the initial chromium masking; e.g. P_G = 20, 30, 50 and 100 μm. Although noises in measurement were superposed on the bottom surface of grooves, straight and steep micro-grooves were formed with the specified pitch of P_G into the DLC coating, as shown in Fig. 14. The etched depth profile becomes a stepwise micro-grooving pattern with the same groove width as 6 μm for varying PG. This assures that various kinds of micro-patterns should be imprinted onto DLC coting only by varying the initial masking pattern.

DISCUSSION

A. CONTROLLABILITY OF OXYGEN PLASMAS

When using the oxygen molecule driven plasma state for etching, the removal rate of DLC coating is retarded and the

etching process terminates in incomplete. On the other hand, oxygen atom driven plasma state is suitable to homogenous etching onto DLC coating with fast removal rate. This difference is attributed to electron density and chemical reaction process during etching process.

Among various processing parameters, RF-voltage and DC-bias have significant influence on this etching process. In general, higher application of RF-power enhances the population of activated oxygen atoms; however, RF-current also increases and leads to unstable plasma state. On the other hand, too much higher or lower DC bias also results in deterioration in etching. Figure 15 depicts the variation of emission spectra for three selections of RF-voltage and DC-bias.

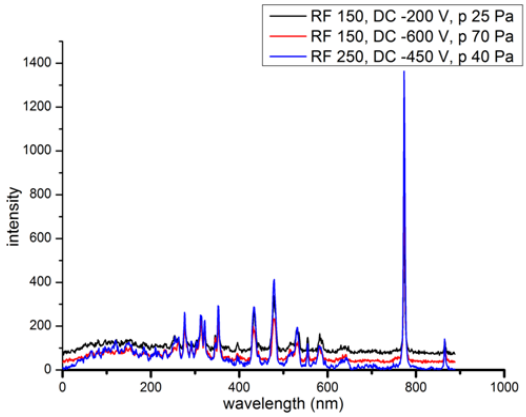

Fig. 15: Variation of emission spectra with varying the RF-voltage and DC-bias.

Among three, RF (250 V) and DC (-450 V) is suitable to activate the oxygen atoms and ions for efficient plasma etching. In parallel with RF and DC, the pressure is also effective to control the plasma state; 40 Pa is recommended to make oxygen plasma etching with high removal rate.

B. PLASMA CHEMICAL REACTION IN ETCHING

Direct reaction between carbon in DLC coating and oxygen atom species in plasma is detected by CO-peaks in the plasma diagnosis. Intensity of these CO-peaks is thought to change itself with duration time during plasma etching process. High peak intensity at the initial stage decreases with duration time in etching. The present plasma diagnosis allows us to make on-line monitoring of these CO-peak intensities during etching. The CO-peak at the wave length of 256.83 nm was selected and on-line monitored with time. Figure 16 describes the variation of this CO-peak intensity with time (t) during the etching process. As expected, the CO-peak becomes nearly constant in the initial stage; carbons in the un-masked DLC film react with the activated oxygen atoms. This peak intensity begins to gradually decrease for $t > 600$ s. When $t = 3000$ s, it approaches to nearly zero; no residual carbon might be present in the un-masked regions. The above online-monitoring is found to be effective to describe the etching behavior with time and to predict the termination of etching process.

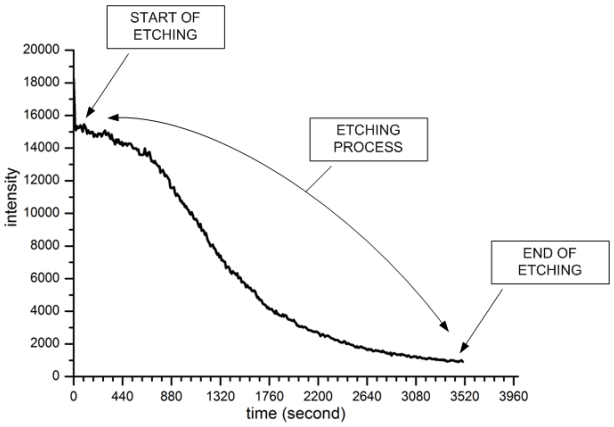

Fig. 16: Variation of detected CO-peak at 256.83 nm with duration time in etching process.

C. COMPARISON OF ETCHING RATE WITH OTHER METHODS

Higher etching rate is preferable to industrial application together with homogeneous etching behavior. After Ref. [17], DLC coating was also removed with the etching rate of 0.5 μm/H by hollow cathode discharging (HCD) method. The present processing enables us to make the etching rate ten times faster: 5 μm/H. In addition, the conventional method in [17] cannot remove the top coat or metallic inter-layers. In the present specimens in Fig. 4, residual chromium was left on the un-masked region after chemical etching in preparation of patterned masking. Amorphous SiC was present as the top coat of DLC films. Hence, these residuals and top-coats are also difficult to be removed by the conventional approaches.

D. ACCURACY OF MICRO-PATTERNING

As had been discussed in Figs. 12-14, a stepwise grooving pattern was fabricated by the present etching into DLC coating, irrespective of the groove width (W_G) and the pitch of patterns (P_G). In particular, when this W_G is more than 3 μm, steep and straight grooving patterns were imprinted into DLC coating down to the bottom of coating with the thickness of 5 μm. This reproducibility in this micro-grooving is favored for homogenous micro- and nano-patterning in relatively large area of mold-dies. Dimensional accuracy on the surface is uniquely determined by the initial pattern to be used. In cases when the initial patterns are formed on the curved surface or in the three-dimensional product surface, oxygen plasma etching is thought to take place uniformly on every spot of surfaces. Since the every surface of substrates is homogeneously covered by high density oxygen plasma sheath, uniform etching advances in the inside of plasma sheath.

When W_G is less than 3 μm and P_G is less than 5 μm, thin walls were forced to be timbered and ashed away; no patterns were left after etching. This deterioration in etching might be closely related to residual stresses in DLC coating. Each thin

wall is forced to be bended with releasing the compressive residual stresses in DLC coating and to be finally timbered in series.

Different from the chemical etching, little anisotropic etching behavior was seen in the present study; i.e. only the un-masked regions of DLC coating were homogeneously removed by activated oxygen atom flux.

CONCLUSION

Precise oxygen-plasma etching with high removal rate of DLC coating is suitable to micro- and nano-patterning onto various DLC-coated tools and mold-dies. Instrumented plasma etching system by plasma diagnosis is also effective to make reliable etching; etching process is in-situ monitored by detection of reactant species so as to terminate the etching process without over-etching to substrate materials. The above effectiveness must be true to micro- and nano-patterning onto the carbon-based coating and bulk materials. The present method is also applied to micro- and nano-patterning onto other carbon-based materials.

Carbon nanotube (CNT) films are micro-patterned to be working as a transparent electrode. Homogeneous ashing and heterogeneous etching by the present approach is also preferable to make surface profile control of diamond-coated tools by reducing the surface roughness of diamond coating.

ACKNOWLEDGEMENTS

Authors would like to express their gratitude to Mr. Y. Sugita (YS Electric Industry, Co., Ltd.) and Mr. H. Morita (Nano-Film Coat, LLC.) for their help in experiments, respectively. This study is financially supported in part by METI-project on semi-dry stamping of nickel battery cans via recyclable DLC-coated tools with the contract number #21231311009, by MEXT-project on advanced DLC coating technology with the contract number of #22560089, and, by the Die and Mold Technology Promotion Foundation project on plasma ashing and etching of DLC coating with the contract number of # 579.

REFERENCES

[1] H. Takahashi, Ed., "Handbook of diamond like carbon coating," NTS-publishing. (2008).

[2] M.J. Lukitsch, A.T. Alpas, "Tribological behavior of aluminum against tungsten doped DLC at elevated temperatures," Abstract of ICMCTF-2011 (2011) 42.

[3] Toyota, Japanese Patent with the contract number of #2011-34429 (2011).

[4] MITI, Supporting Industry Project on high qualification of mold-die technology for fabrication of optical elements. (2009).

[5] T. Aizawa, K. Itoh, T. Inohara, "Imprinting of patterns onto polymers and oxide-glasses via fine micro-stamping," Proc. 6th ICOMM Conference. (2011) 77-82.

[6] T. Aizawa, K. Itoh, T. Fukuda, "Fine micro-stamping system for micro-pattern printing onto polymers and glasses," Proc. 10th ICTP Conference (2011) 1097-1102.

[7] T. Inohara, T. Aizawa, "Development of pico-second laser machining for multi-dimensional micro-patterning," Final Report of METI-Project for Supporting Industries. (2011).

[8] T. Aizawa, T. Inohara, "Multi-dimensional micro-patterning onto ceramics by pico-second laser machining," Research Report, Shibaura Institute of Technology. 55-3 (2012) (in press).

[9] T. Aizawa, T. Inohara, Japanese Patent with the contract number of # 2011-212046 (2011).

[10] T. Aizawa, Japanese patent with the contract number of # 2010-045110 (2010).

[11] T. Aizawa, "Micro-patterning onto diamond like carbon coating via RF-DC oxygen plasma etching," Proc. 5th SEATUC Conference. (2011) 425-428.

[12] T. Aizawa, Y. Sugita, "High-dense plasma technology for etching and ashing of carbon materials," Research Report, Shibaura Institute of Technology. 55-2 (2011) 13-22.

[13] T. Aizawa, T. Fukuda, Japanese patent with the contract number of #2010-045110 (2010).

[14] National Institute of Science & Technology, NIST Atomic Spectra Database (http://physics.nist.gov/cgi-bin/ASD/lines1.pl.

[15] A. Cuesta, A. Mart´ınez-Alonso, J.M.D. Tasco´n, "Carbon reactivity in an oxygen plasma: a comparison with reactivity in molecular oxygen," Carbon. 39 (2001) 1135–1146.

[16] U. Cvelbar, et. al., "Inductively coupled RF oxygen plasma characterization by optical emission spectroscopy," Vacuum 82 (2008) 224–227.

[17] T. Okimoto, T. Kumakiri, H. Tamagaki, "Application of hollow cathode plasmas to SiOx coating," Future: Advanced thin film technology in Research Report of KOBELCO. 52 (2) (2002) 13-18.